CHEMISTRY
A European Journal

A Journal of
ChemPubSoc Europe

Accepted Article

Title: Evaluation of the Medicinal Potential of Two Ruthenium(II) Polypyridine Complexes as One- and Two-Photon Photodynamic Therapy Photosensitizers

Authors: Jeannine Hess, Huaiyi Huang, Adrian Kaiser, Vanessa Pierroz, Olivier Blacque, Hui Chao, and Gilles Gasser

To be cited as: *Chem. Eur. J.* 10.1002/chem.201701392

Link to VoR: http://dx.doi.org/10.1002/chem.201701392

Supported by
ACES

WILEY-VCH

10.1002/chem.201701392

Evaluation of the Medicinal Potential of Two Ruthenium(II) Polypyridine Complexes as One- and Two-Photon Photodynamic Therapy Photosensitizers

Jeannine Hess,[a,#] Huaiyi Huang,[a,b,#] Adrian Kaiser,[a] Vanessa Pierroz,[a] Olivier Blacque,[a] Hui Chao,[b,*] Gilles Gasser[c,*]

[a] *Department of Chemistry, University of Zurich, Winterthurerstrasse 190, CH-8057, Zurich, Switzerland.*

[b] *School of Chemistry, Sun Yat-Sen University, Guangzhou 510275, P. R. China.*

[c] *Chimie ParisTech, PSL Research University, Laboratory for Inorganic Chemical Biology, F-75005 Paris, France.*

[#] these authors have contributed equally to the work.

[*] *Corresponding authors.* E-mail: ceschh@mail.sysu.edu.cn, Tel: 86 20 8411 0613; E-mail: gilles.gasser@chime-paristech.fr Tel: +33 1 44 27 56 02, WWW : www.gassergroup.com.

KEYWORDS*:* Cancer, Medicinal Inorganic Chemistry, Photodynamic Therapy (PDT), Photosensitizers, Ruthenium(II) Complexes

10.1002/chem.201701392

Abstract: Two $[Ru(phen)_2dppz]^{2+}$ derivatives (phen = 1,10-phenantroline, dppz = dipyrido[3,2-a:2′,3′-c]phenazine) with different functional groups on the dppz ligand [dppz-7,8-$(OMe)_2$ (**1**), dppz-7,8-$(OH)_2$ (**2**)] have been synthesized, characterized and investigated as photosensitizers (PSs) for photodynamic therapy (PDT) against cancer. Both complexes showed intense red phosphorescence and promising singlet oxygen ($^1O_2$) quantum yields of 75 % (**1**) and 54 % (**2**), respectively, in acetonitrile. **1** (log$P_{o/w}$ = -0.52, 2.4 nmol Ru per mg protein) was found to be more lipophilic, having also a higher cellular uptake efficiency compared to **2** (log$P_{o/w}$ = -0.20, 0.9 nmol Ru per mg protein). **1** localized evenly in HeLa cells whereas **2**, was mainly visualized in the cell membrane by confocal microscopy. In the dark, **1** (IC_{50} = 36.2 μM) was found to be more toxic than **2** (IC_{50} > 100 μM) on HeLa cells monolayer. Importantly in view of PDT applications, both complexes were found to be non-toxic towards multicellular HeLa spheroids (IC_{50} > 100 μM). Upon one-photon irradiation (420 nm, 9.27 $J{\cdot}cm^{-2}$), **1** exhibited higher phototoxicity (IC_{50} = 3.1 μM) than **2** (IC_{50} = 16.7 μM) on HeLa cell monolayers. When two-photon irradiation (800 nm, 9.90 $J{\cdot}cm^{-2}$) was applied, only **1** (IC_{50} = 9.5 μM) was found to be active toward HeLa spheroids. This study demonstrates that the functional group on the intercalative ligand has a strong influence on the cellular localization and anticancer activity of Ru(II) polypyridyl complexes.

10.1002/chem.201701392

Introduction

Over the recent years, photodynamic therapy (PDT) has expanded the range of available methods to treat certain types of cancer (i.e. lung, bladder, and urinary tumors).[1] PDT works through the light activation of a photosensitizer (PS), which generates reactive oxygen species (ROS) that are toxic. These ROS then ultimately lead to cancer cell death, with only minimal damage to normal tissues.[2] More specifically, the light-activated PS reacts with oxygen present in tissue ($^3O_2$) to generate ROS through two main types of reaction pathways.[3] In type I reaction, the triplet-state of the PS directly transfers an electron to $^3O_2$ or other oxygen-containing species and generates radical ions. In type II reaction, the excited state of the PS reacts with ground-state molecular oxygen, namely $^3O_2$, *via* an excited-state energy transfer to generate extremely reactive singlet oxygen ($^1O_2$). Due to its high reactivity, $^1O_2$ causes oxidative damage in different cellular components (i.e. plasma membrane, endoplasmic reticulum, mitochondria, lysosome, nucleus, etc.).[4] Interestingly, PDT can also induce vasoconstriction and blood flow stasis resulting in anoxia and subsequent cell death inside tumours.[5] To date, the most commonly used PS in clinical studies is Photofrin. Photofrin has been clinically approved to treat bladder cancer, early stage lung cancer, oesophageal cancer and early non-small cell lung cancer.[6] However, besides tedious synthesis and purification, as well as poor water solubility, Photofrin is also associated with a pronounced and prolonged generalised skin photosensitivity and only little initial selectivity.[6]

Although most of the approved PSs for PDT are porphyrin- or phtalocyanine-based organic molecules, metal complexes can also be employed as excellent PS candidates.[7] Due to

10.1002/chem.201701392

their ideal physico-chemical properties (i.e. intense luminescence, large Stokes shifts, high chemical stability and photo-stability, relatively long phosphorescent lifetimes, high water solubility and high $^1O_2$ production),[8] Ru(II) polypyridyl complexes have recently emerged as a promising alternative to the current PSs. As a highlight, $[Ru(dmb)_2(IP\text{-}TT)]^{2+}$, (TLD-1433, dmb = 4,4′-dimethyl-2,2′-bipyridine, IP-TT = 2-(2′,2″:5″,2‴-terthiophene)-imidazo[4,5-f][1,10]phenanthroline, **Scheme 1**) just entered into clinical trials for PDT treatment of non-muscle invasive bladder cancer.[9] Of note, in recent years, several DNA intercalating Ru(II) polypyridyl complexes have been reported as effective DNA photo-cleavage agents and photosensitizes for PDT.[10]

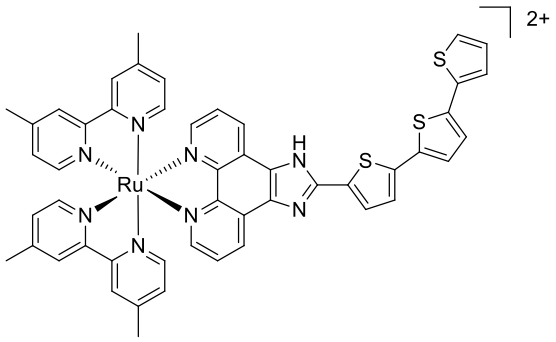

TLD-1433

Scheme 1. Chemical structure of TLD-1433 ($[Ru(dmb)_2(IP\text{-}TT)]^{2+}$, dmb = 4,4′-dimethyl-2,2′-bipyridine, IP-TT = 2-(2′,2″:5″,2‴-terthiophene)-imidazo[4,5-f][1,10] phenanthroline).

Despite the currently approved PDT agents are excited by one-photon (OP) excitation using a high energy laser beam, they have only a limited tissue penetration since short wavelengths are employed. In order to tackle this drawback, two-photon PDT (TP-PDT) agents have recently emerged as attractive alternatives to the currently approved PSs.[11] Contrary to one-photon PDT (OP-PDT), TP-PDT uses low energy near-infrared laser

irradiation, which not only allows for deeper tissue penetration, but is also less invasive towards normal cells. This results in reduced photo-bleaching of the PSs.[12] It should be noted that OP-PDT uses higher photon energy but can be carried out with low power lasers and LEDs, whereas TP-PDT uses lower photon energy but requires higher power lasers. In view of TP-PDT applications, viable PSs must have a high efficiency for two-photon absorption (TPA); a property that is quantified by the two-photon absorption cross-section value (σ_2).

Theoretically speaking, the higher the TP cross-sections is, the better the TP PDT efficiency should be. However, one has also to consider the balance between hydrophilicity and hydrophobicity, the singlet oxygen generation efficiency as well as the cellular uptake efficiency of the PS. Although some conjugated porphyrins showed significant two-photon absorption, the σ_2 values of clinical used porphyrins are insufficient for adequate clinical applications in TP-PDT.[13] Among the different PSs that have been tested for TP-PDT, Ru(II) polypyridyl complexes (σ_2 values ≈ 62-250 GM) were found to be excellent candidates, with σ_2 values much higher than porphyrins.[10g, 14] However, the physical and chemical properties of Ru(II) complexes can still be improved by lowering their dark cytotoxicity or by increasing their photo-index (PI).[14a, 15]

Cancer cells divide and multiply much faster than normal cells. Targeting the DNA replication machinery thus more severely affects cancer cells in relation to normal tissues, and DNA targeting anticancer drugs such as cisplatin or doxorubicin are widely used in chemotherapy.[16] Similarly, PSs preferentially localizing in the cell nucleus provide an outstanding opportunity to target the replication system and selectively affect cancer cells.

$[Ru(phen)_3]^{2+}$ (phen = phenanthroline) was the first Ru(II) complex to be found to bind to the minor groove of double helix DNA.[17] Subsequently, Barton *et.al* reported the introduction of extended planar ligand systems, such as dppz (dppz = dipyrido[3,2-a:2′,3′-c]-phenazine) in $[Ru(bpy)_2(dppz)]^{2+}$ (bpy = 2,2'-bipyridine), which showed a significant increase in DNA binding efficiency. Interestingly, the phosphorescence of $[Ru(bpy)_2(dppz)]^{2+}$ is quenched in aqueous solution. However, upon the addition of DNA, the dppz ligand can rapidly intercalate between the base pairs of DNA and the Ru(II) complex emits intense red phosphorescence. As a result, $[Ru(bpy)_2(dppz)]^{2+}$ is known as an excellent DNA intercalative "light-switch" complex.[18]

It has been shown that the physico-chemical properties of Ru(II) polypyridyl complexes can be rationally designed to be water soluble or water insoluble, photo-stable or photo-unstable, or to have long or short triplet lifetimes.[19] For example, $[Ru(bpy)_2dppn]^{2+}$ (dppn = benzo[*i*]dipyrido[3,2-a:2′,3′-h]quinoxaline) exhibits much higher lipophilicity and dark toxicity than $[Ru(bpy)_2phen]^{2+}$ and $[Ru(bpy)_2dppz]^{2+}$.[20] Worthy of note, McFarland reported that the same compound had a very low dark toxicity in a different cell line, namely HL-60 promyelocytic cell line.[21] Moreover $[Ru(phen)_2dppz]^{2+}$ presents enhanced light switching properties and stronger photoluminescence intensities than $[Ru(bpy)_2dppz]^{2+}$ when binding to DNA.[22] However, the impact on the photochemistry and phototoxicity by changing the substituents on the dppz ligand has only been sparingly studied. Some of us have reported $[Ru(bpy)_2(dppz)]^{2+}$ derivatives bearing different mono functional groups on the dppz ligand as potential PSs in one-photon PDT[23] but there is undoubtedly a lack of studies on this topic.

In this work, we report on the synthesis, characterization, and biological evaluation of two substitutionally inert $[Ru(phen)_2(dppz)]^{2+}$ derivatives with different functional groups on the dppz ligand (dppz-7,8-$(OMe)_2$ (**1**), dppz-7,8-$(OH)_2$ (**2**), **Scheme 2**) as PSs for one- and two-photon PDT. The purpose of the conducted research was to investigate the influence of small structural ligand modifications on the photochemical and biological behaviour of Ru(II) complexes. The distribution coefficients ($\log P_{o/w}$), two-photon absorption cross-section, singlet oxygen generation quantum yield, cellular distribution, cellular uptake efficiency and stability in human plasma were investigated. Finally, the dark and light cytotoxic activities of these two complexes was investigated on cervical cancer (HeLa) cell monolayer and multicellular HeLa spheroids for OP-PDT and TP-PDT.

Results and discussion

Synthesis and characterization.

The synthetic route for complexes **1** and **2** is outlined in **Scheme 2** (the ligand synthesis can be found in the Supporting Information **Figure S1**)**.** In an initial step, the two nitro groups of 1,2,-dimethoxy-4,5-dinitrobenzene (**1a**) were reduced using Pd/C and H_2 to obtain 1,2-dimethoxy-4,5-diaminobenzene (**1b**). The dppz-7,8-$(OMe)_2$ (**1c**) intermediate was then obtained after Schiff base condensation of **1b** with 1,10-phenantroline in 73% yield. In the next step, the first ruthenium complex **1** was isolated in 60% yield after refluxing **1c** with $[Ru(phen)_2Cl_2]\cdot 2H_2O$ in $EtOH/H_2O$. Attempts were made to synthesize **1** by reacting $[Ru(phen)_2(phen\text{-}dione)_2]\cdot 2H_2O$ directly with **1b**. However, the reaction yield for the desired complex was overall low. In the last reaction step, the two methyl groups of

10.1002/chem.201701392

1 were cleaved using an aqueous solution of 48% HBr to finally afford complex **2** in moderate yield (33%). Both **1** and **2** were unambiguously characterized by ^{1}H and ^{13}C NMR spectroscopy, mass spectrometry and elemental analysis (see Supporting Information **Figures S2-S7**).

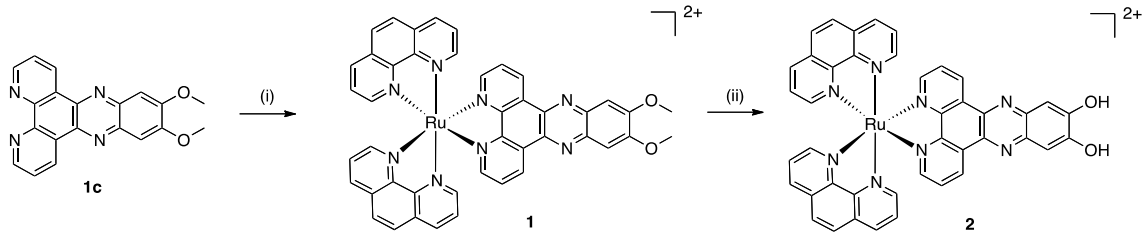

Scheme 2. Reagents and conditions: (i) $[Ru(phen)_2Cl_2]\cdot 2H_2O$, $EtOH/H_2O$, reflux, o.n. 40%; (ii) Acetic acid, aq. 48% HBr, o.n., 33%.

Crystallography.

The molecular structures of **1** and its planar ligand **1c** were confirmed by single crystal X-ray diffraction (**Figure 1, Table S1**). In the crystal structure of **1** the Ru(II) center adopts a distorted octahedral coordination geometry with two phenanthroline and one dppz-7,8-$(OMe)_2$ ligands acting as N,N-bidentate ligands. The Ru–N bond distances and the N–Ru–N bond angles fall in normal ranges: 2.040(6) – 2.115(5) Å and 80.72(19) – 81.5(2)°, respectively (a search in the Cambridge Database revealed an average Ru–N bond distance of 2.070 Å with a standard deviation of 0.024 Å obtained on 46 structures containing the Ru(dppz) fragment; similarly an average N–Ru–N bond angle of 79.2° was found in the same reported structures with a standard deviation of 1.0°).

10.1002/chem.201701392

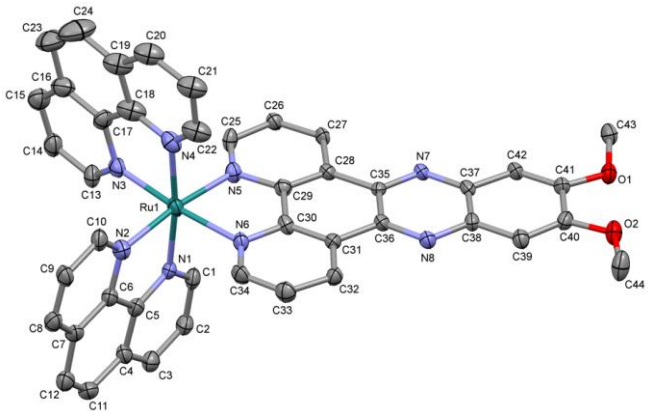

Figure 1. Molecular structure of **1** with an atomic numbering scheme (counter-ions, water molecules and hydrogen atoms excluded for clarity).

The three η^2 ligands are perpendicular to each other as indicated by the dihedral angles of 85.3(3), 89.1(3) and 89.3(3)° calculated between the mean planes. The presence of three planar aromatic ligands is favourable to ring interactions in the solid state; some of them with centroid-centroid distances smaller than 4 Å can be considered as short π-π interactions. The smallest distance was found to be 3.558(4) Å between two ligands almost parallel to each other (4.9(3)° between the mean planes). The three-dimensional framework formed by the π-π interactions created large tunnels running along the a and b axes in which isolated water molecules are located, and a narrower tunnel along the c axis where ClO_4^- ions are observed, linked to the Ru(II) molecules via weak C–H···O hydrogen bonds (the shortest H···O and C···O distances are 2.33 and 3.14(2) Å, respectively) (**Figures S8-S10**). The crystal structure of **1c** revealed that the free ligand dppz-7,8-$(OMe)_2$ adopts the same conformation with similar structural parameters as in the crystal structure of **1** where it is coordinated to a Ru(II) centre (**Figure S11**). The molecule is nearly planar, including the

carbon atoms of the OMe groups. Solvent molecules of chloroform co-crystallized with the main species. They are linked together via weak C–H···N and C–H···Cl hydrogen bonds. In addition, the planar dppz molecules are packed along the c axis by π-stacking interactions and the shortest centroid-centroid distance found in the crystal structure is 3.488(2) Å between two parallel molecules (the dihedral angle between the corresponding mean planes is 6.11(14)°) (**Figures S12-S13**).

Photophysical properties.

The photophysical properties of the two complexes were evaluated to gain further insight in their potential as PDT PSs. **1** and **2** showed a typical metal-to-ligand charge-transfer (MLCT) absorption band for Ru(II) complexes in the visible region (400-500 nm) (**Figure S14**).[24] The absorption of **2** was slightly red-shifted compared with **1**. Upon excitation with 420 nm light, **1** and **2** showed intense emission bands around 620 nm in CH_3CN (**Figure S15**), similarly to other polypyridyl Ru(II) complexes.[23b] In PBS solution, the emission signals were significantly quenched by water. The phosphorescence quantum yields (Φ_{em}) evaluated in air-equilibrated CH_3CN (**Table 1**) were calculated by comparison with $Ru(bpy)_3^{2+}$ in methanol (Φ_{em} = 4.2 %).[25] The quantum yield values in acetonitrile of **1** (Φ_{em} = 2.8 %) and **2** (Φ_{em} = 1.7 %) were found to be comparable with the unsubstituted complex $[Ru(phen)_2dppz]^{2+}$ (Φ_{em} = 3.3 %), meaning that the functional group did not have an influence on the excited state.[26] The phosphorescence emission lifetimes in degassed CH_3CN were much longer than in aerated CH_3CN (**Figure S16**). **1** showed longer luminescence lifetimes in both aerated (325 ns) and degassed (645 ns) CH_3CN solutions

than **2** (109 ns and 220 ns, respectively) (**Table 1**).

Table 1. Photophysical data for the complexes in CH_3CN at room temperature.

	λ_{ex} /nm	λ_{em} /nm	Φ_{em} /%	Lifetime /ns air	Lifetime /ns degassed	Φ_{Δ} /% PBS	Φ_{Δ} /% CH_3CN	log P
1	420	620	2.8	325	645	3	75	-0.52
2	420	621	1.7	109	220	5	54	-0.20

The presence of oxygen therefore had a significant influence on the lifetime of the excited state for both of the complexes. These results confirm that molecular oxygen in its ground state is able to interact with the triplet excited state of Ru(II) complexes. The TPA cross-section (σ_2) of **1** and **2** from 720 to 850 nm are shown in **Figure 2** and the slope of integrated emission intensity as a function of laser power was found to be around 2 (**Figure S17**).

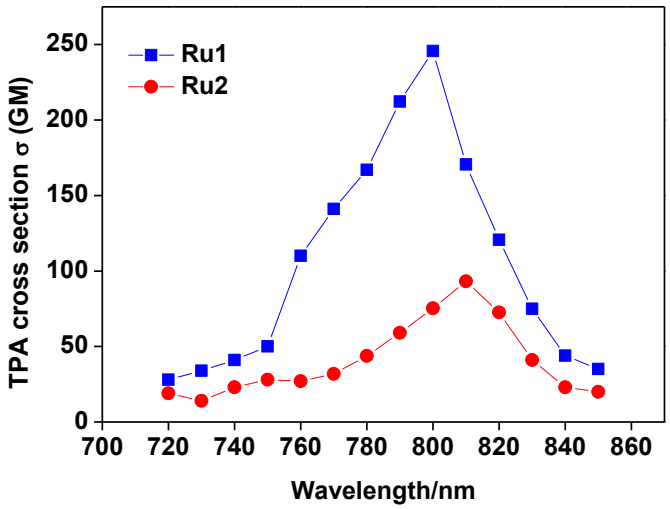

Figure 2. TPA cross section of **1** and **2** in methanol.

The largest TPA of **1** (245 GM) and **2** (93 GM) was found to be around 800 nm. These values are comparable with other Ru(II) polypyridyl complexes previously reported for TP-PDT.[10g, 14] Worthy of note, the TPA values of **1** and **2** were much higher than the clinical approved photosensitizer H_2TPP (< 20 GM at 800 nm).[13a]

Singlet oxygen generation.

A quantitative evaluation of the singlet oxygen $^1O_2$ ($^1\Delta_g$) production upon irradiation at 420 nm was performed to assess the potential of these complexes as PDT PSs.[27] The formation of $^1O_2$ was monitored in an assay based on its reaction with an imidazole derivative to form a trans-annular peroxide adduct, which is able to quench the absorbance of *p*-nitrosodimethyl aniline (RNO).[28] The measurements of $^1O_2$ generation quantum yield were carried out in both PBS (with 10 mM histidine) and acetonitrile (with 12 mM imidazole) solutions. The $^1O_2$ production quantum yields were evaluated by comparison with the reference molecule phenalenone (Φ ($^1\Delta_g$) = 95%).[29] The results obtained are shown in **Table 1**. Both complexes exhibited 10 times higher singlet oxygen generation efficiency in acetonitrile than in PBS. These results are comparable with previously reported data on similar Ru(II) complexes.[11]

Stability of 1 and 2 in human plasma.

In order to assess the compatibility of complexes **1** and **2** in physiological conditions, their stability in human plasma was evaluated using an adapted method performed previously for other Ru^{II} complexes.[23a] Although **1** and **2** are structurally similar polypyridyl Ru(II)

10.1002/chem.201701392

complexes, their stability greatly differ. **1** was found to be stable in human plasma upon incubation at 37 °C for 48 h when compared to the internal standard (diazepam) (**Figure 3, Figures S18-S19**). In contrast, compound **2** was found to decompose significantly in human plasma. After 24 h and 48 h incubation at 37 °C, only 32% and 19%, respectively, of complex **2** remained intact (**Figure 3, Figures S20-S21**).

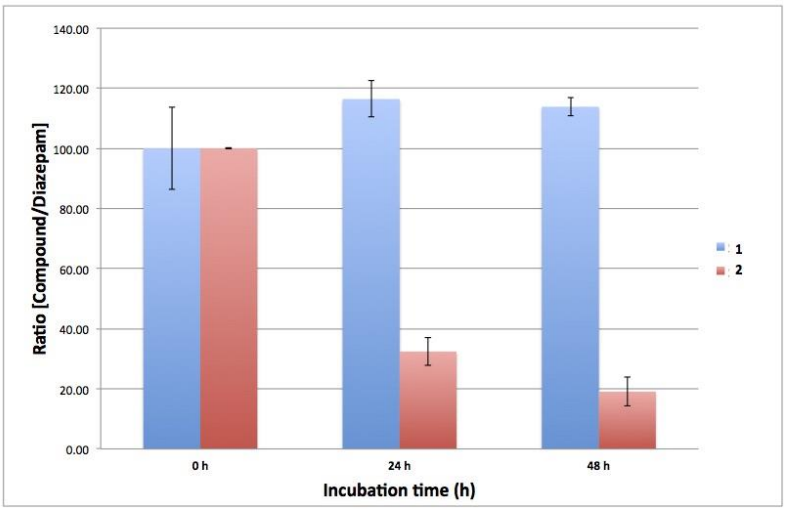

Figure 3. Ratio [%] of **1** and **2** to diazepam (internal standard) at different time intervals (0 h, 24 h, 48 h) in human plasma. The UPLC chromatograms (375 nm) of complexes **1** and **2** as well as the chromatograms of **1** and **2** in the presence of the internal standard (diazepam) after 0 h, 24 h and 48 h of incubation in human plasma can be found in the supporting information (**Figure S17-S20**).

These results are in line with previously performed human plasma stability experiments on similar Ru(II) complexes. As investigated previously, a similar [Ru(II)(bipy)2-dppz-7-hxdroxyl]$^{2+}$ complex partially decomposed after 4 h of incubation in human plasma.[23a] These results demonstrate that only slight structural modifications of the ancillary functional groups can have a dramatic impact on the stability of Ru(II) polypyridyl

10.1002/chem.201701392

complexes.

Hydrophobicity Measurements.

The lipophilicity of a compound is well-known to be related to its cellular uptake and anticancer efficiency.[30] Lipophilicity can be quantitatively evaluated by the determination of its log$P_{o/w}$ value, where $P_{o/w}$ is the partition coefficient between octanol and water. Log$P_{o/w}$ determination revealed that **2** (log$P_{o/w}$ = -0.20) was more lipophilic than **1** (log$P_{o/w}$ = -0.52) (**Table 1**). The log$P_{o/w}$ value of **2** was also higher than $[Ru(bpy)_2dppz\text{-}OH]^{2+}$ (log$P_{o/w}$ = -0.45) with bpy as the auxiliary ligand and the same mono-functionalized dppz ligand,[38] whereas the difference between $[Ru(bpy)_2dppz\text{-}OMe]^{2+}$ (log$P_{o/w}$ = -0.42) and $[Ru(bpy)_2dppz\text{-}OH]^{2+}$ (log$P_{o/w}$ = -0.45) was minor.[38]

Dark- and photo-toxicity.

After having established the photo-physical and chemical properties of complexes **1** and **2**, their dark and photo-toxicity was initially tested on cervical cancer HeLa cell monolayers and the non-cancerous MRC-5 cell line (**Table 2**). The cells were exposed to the different compounds (**1**, **2**, ALA, Cisplatin) for 4 h. This was followed by replacement with fresh medium and incubation in the dark for 44 h.

10.1002/chem.201701392

Table 2. IC_{50} values (μM) and phototoxic index (PI) of HeLa cancer cell monolayer, multicellular HeLa cancer cell spheroids and non-tumorigenic control cell line MRC-5.

Compound	**MRC-5 normal cells**			**2D HeLa cell monolayer**			**3D multicellular HeLa spheroids**				
	Dark[a]	OP[a]	PI	Dark[a]	OP[b]	PI	Dark	OP[c]	PI	TP[d]	PI
1	39.2 ± 1.6	5.8 ± 0.9	6.7	36.5 ± 3.0	3.1 ± 0.6	11.7	104 ± 7.9	32.5 ± 6.8	3.2	9.5 ± 2.5	11
2	>100	24.5± 2.5	> 4.1	>100	16.7 ± 2.6	> 5.9	>100	>100	n.a[e]	>100	n.a[e]
ALA	>200	>200	n.a.	>200	154.8 ± 14.5	>1	>200	>200	n.a[e]	>200	n.a[e]
Cisplatin	17.4 ± 1.6	18.8 ± 1.9	n.a.	28.3 ± 3.1	29.5 ± 2.6	n.a[e]	65.6 ± 7.6	71.4 ± 8.2	n.a[e]	69.5 ± 5.4	n.a[e]

[a]4 h drug exposure followed by 44 h incubation in the dark. [b]4 h drug exposure, changed with fresh medium followed by light irradiation (420 nm, 9.27 J cm^{-2}) and then 44 h incubation in the dark. [c]24 h drug exposure followed by irradiation (450 nm, 10.00 J cm^{-2}) and then 48 h incubation at 37 °C, 5% CO_2. [d]24 h drug exposure followed by irradiation at 800 nm (9.90 J cm^{-2}) and then 48 h incubation at 37 °C, 5% CO_2. [e]Not applicable.

Cisplatin was used as a positive control for the dark cytotoxicity. **1** was found to be more cytotoxic (IC_{50} = 36.5 μM) than **2 (**IC_{50} > 100 μM) for HeLa cells treated for 4 h in the dark. Of note, it was impossible to obtain an exact IC_{50} value of **2** due to precipitation of the complex at concentrations exceeding 100 μM. For comparative purposes, the dark toxicity of **1** (36.5 μM) after 4 h incubation was significantly higher than the non-functionalized Ru(II) complex $[Ru(phen)_2dppz]^{2+}$ (152.1 μM) even after much longer drug exposure (48 h).[30] The introduction of two –OMe groups on the dppz ligand thus clearly results in an enhanced dark toxicity. In contrast, introducing –OH groups as in complex **2** did not result in a significant change in dark toxicity.

We then tested the photo-toxicity of both complexes towards cancer cells after 4 h incubation in the dark, washing of the cells, replacement with fresh medium and then

irradiation at 420 nm for 20 min (9.27 J cm^{-2}). The cells were further incubated for 44 h before determining the cell viability. The clinically approved PDT PS 5-aminolevulinic acid (ALA), which is a precursor in protoporphytin IX biosynthesis, was used as a positive control.[31] Photo-toxicity experiments were carried out using the following protocol: 4 h incubation, change to fresh medium, 20 min light irradiation and 44 h incubation in the dark. The phototoxicity of **1** (IC_{50} = 3.1 μM) on HeLa cell monolayers was found to be higher than the one of **2** (IC_{50} = 16.7 μM). Due to different experimental conditions used for the determination of the dark cytotoxicity, we can only compare the IC_{50} values to Ru(II) complexes with bpy as the auxiliary ligand and mono-functionalized group on dppz ligand. **1** (IC_{50} = 3.1 μM) was slightly more toxic than $[Ru(bpy)_2dppz\text{-}OMe]^{2+}$ (IC_{50} = 5.5 μM).[23a] The higher singlet oxygen generation quantum yield of **1** seemed to result in higher PDT effect on cancer cells monolayer upon 420 nm light irradiation. Importantly, both Ru(II) complexes were found to be more effective than 5-ALA (IC_{50} = 154.8 μM, PI >1). The relatively low PI value obtained for 5-ALA was due to lower concentrations used in this assay if compared to the dose typically applied in clinical PDT treatments (about 1 mM), at which 5-ALA has a higher PI value.[32] The highest concentration of 5-ALA tested in our assay was 200 μM, following a previously used protocol,[27] which was sufficient to allow for a direct comparison to the investigated Ru(II) complexes.

In vitro cultured cancer cell monolayers have a different behavior compared with cancer cells growing within solid tumors. The latter are generally less sensitive to chemotherapeutics.[33] As an example, doxorubicin is highly toxic towards cancer cell monolayers but relatively inactive on cancer cells present in solid tumors. This difference

10.1002/chem.201701392

reflects reduced drug penetration depth and pathophysiological differences or relatively slower cell cycling in solid tumors.[33] In recent years, *in vitro* 3D multicellular tumor spheroid (MCTS) cell culture systems have received increasing interest in anticancer drug evolution. MCTSs can be used a cell model to study the tissue penetration of fluorescent drugs. MCTSs can generate an extracellular matrix (ECM) and mimic metabolic and proliferative gradients, hypoxic areas, as well as the multidrug resistance found in solid tumors.[34] One of the most important advantages of TP light is its deeper tissue penetration compared to OP light. In this respect, MCTSs function as a better cell model for TP photodynamic therapy studies than cancer cell monolayer. Thus, HeLa MCTSs were selected to investigate the TP-PDT anticancer activity of our Ru(II) polypyridyl complexes.[35]

The IC_{50} values of **1** (104 μM) and **2** (> 100 μM) in the dark on 400 μm HeLa MCTSs were found to be above 100 μM. Upon TP irradiation (800 nm, 9.90 J cm^{-2}), the IC_{50} values of **1** decreased to 9.5 μM, approximately 3 times lower than the IC_{50} value obtained for OP irradiation (IC_{50} = 32.5 μM, 450 nm, 10.0 J cm^{-2}). Though **2** generates higher singlet oxygen quantum yield (5 %) in PBS than **1** (3 %), **2** was found totally inactive against MCTSs (IC_{50} > 100 μM, **Table 2**) under both OP and TP irradiation. These data demonstrate a significant difference between the phototoxic properties of **1** and **2** on HeLa cell monolayers and HeLa MCTSs. Thus, we carried out cellular localization and cell uptake studies to obtain some more insights into the mechanism of cell death upon light irradiation.

10.1002/chem.201701392

Intracellular localization.

To understand the phototoxic behaviour of the two Ru(II) complexes, we firstly quantified the cellular amount of ruthenium by inductively coupled plasma mass spectrometry (ICP-MS). The sensitivity of ICP-MS makes it a practical method to detect and identify metal-based complex within cells.[36] After 4 h incubation, the amount of **1** (2.4 nmol Ru per mg protein) within HeLa cells was higher than the one of **2** (0.9 nmol Ru per mg protein). This difference in cellular localization can be regarded as a possible cause of the significant difference in the dark cytotoxicity of **1** and **2**.

In addition to ICP-MS, confocal microscopy imaging of **1** and **2** under OP (420 nm) and TP (800 nm) excitation was also performed. The Ru complexes that were not internalized at this time point were replaced with fresh medium. As shown in **Figure S22**, **1** homogeneously distributes within the cytoplasm and nucleus, while **2** locates mostly at the outer surface of HeLa cells, as visualised under both OP and TP excitation. Subsequently, the exact localization of **1** and **2** was determined by co-staining with commercial organelle dyes. We incubated HeLa cells with complexes **1** and **2** (50 μM, 4 h) and organelle dyes (30 min) in the dark and then imaged them with a confocal microscope. As shown in **Figure 4**, the red signal of **1** overlays with both the fluorescent signal of Hoechst 33342 (nucleus dye) and of Mitotracker green (MTG, mitochondria dye). On the contrary, **2** was found to locate at cell membranes. The luminescence of **2** overlays well with the one of the green membrane cell dye Dio. No overlay of luminescence could be observed with Hoechst 33342.

10.1002/chem.201701392

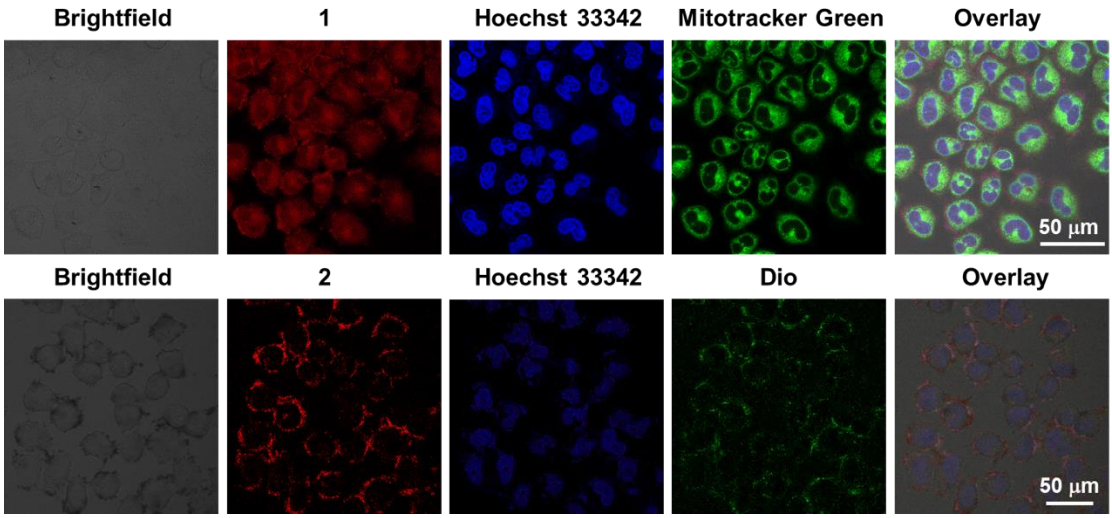

Figure 4. Cellular localization of **1** and **2**. HeLa cells were firstly incubated with **1** or **2** (50 µM, 2 h) and then incubated with commercial dyes for another 30 min. Scale bar = 50 µm. Excitation wavelengths: 458 nm (**1** and **2**), 488 nm (Dio), 488 nm (MTG green) and 405 nm (Hoechst 33342). Emission filter: 600 ± 20 nm (for **1** and **2**), 520 ± 20 nm (for MTG), 500 ± 20 nm (Dio) and 460 ± 20 nm (for Hoechst 33342).

Overall, the cellular distribution of **1** was found to be similar to the one of the Ru(II) analogue $[Ru(bpy)_2dppz\text{-}OMe]^{2+}$ with a mono-functionalised dppz ligand previously reported by our group. However, the cell membrane localization property of **2** was relatively surprising since only Ru(II)-dppz complexes with alkyl ether chains have been reported to image cell membranes.[37] In this previous study, the more hydrophobic complex with long alkyl ether chains (R = C_6H_{13}) was found to localise in cell membranes.[37] Complex **2** seems to be stuck at the cell membrane due to strong interaction with lipid bilayer, which result in reduced uptake inside cancer cells. Thus the higher dark cytotoxicity of **1** compared to **2** may be due to a better cell uptake efficiency of **1** than **2**.

10.1002/chem.201701392

In regards to cellular localization measured by fluorescent microscopy, a note of caution must be applied since in view of their luminescent quenching properties in aqueous solution, **1** and **2** can only be visualized when present in hydrophobic environments, such as in the cell membranes or when bound to proteins or DNA of HeLa cells. Therefore, it is not excluded that these compounds are located in other compartments where they remain undetected. Such an observation has been previously made by us and others.[38]

Apart from HeLa cell monolayers, we were also interested in the difference between the OP and TP cell imaging properties of **1** and **2** on cancer cell spheroids. The cellular uptake efficiency may be quite different between cancer cell spheroids and cancer cell monolayers due to the lower cell penetration of a compound. As shown in **Figures 5** and **6**, the MCTS penetration ability of **1** (50 μM, 12 h) was much higher than the one of **2** (50 μM, 12 h) under the same experimental conditions.

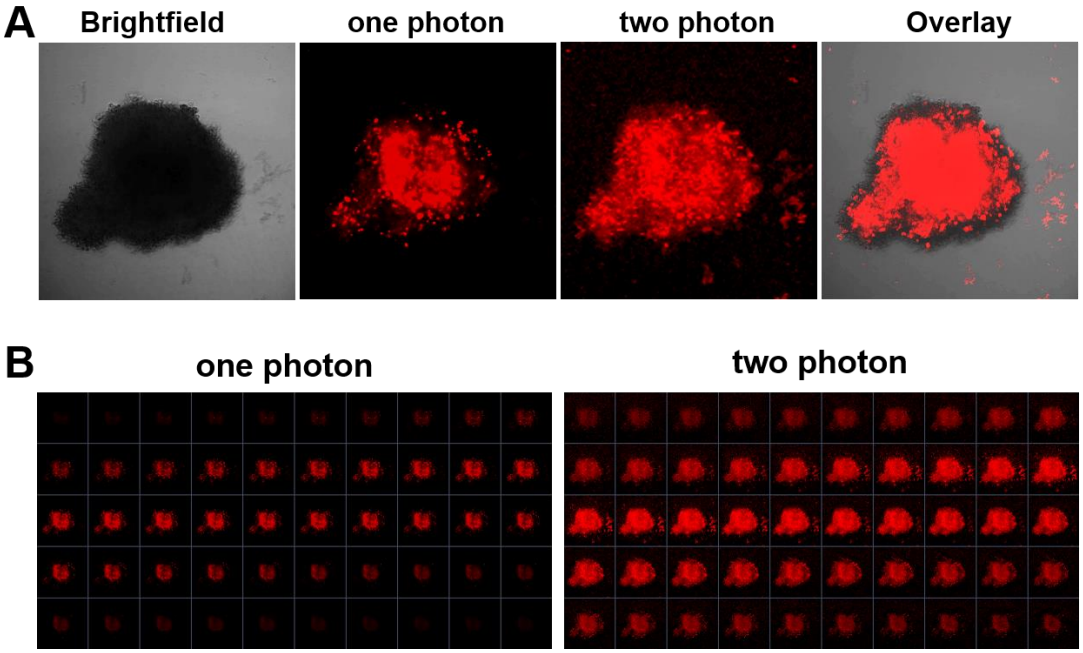

Figure 5. (A) 1P and 2P images of **1** (50 μM) after incubation with HeLa spheroids for 12 h. (B) Z-

stack images of the same HeLa spheroids captured every 5 μm along the Z-axis. Excitation wavelengths: 800 nm (**1** and **2**), Emission filter: 600 ± 20 nm (for **1** and **2**).

2 was found to only stain the outer sphere of HeLa spheroid as confirmed by Z-scan images (**Figure 6B**). No signal from the centre of HeLa MCTSs could be observed. The low penetration of **2** into MCTSs is coherent with its observed preferred localization on cell membranes, thus making it a poor candidate for TP-PDT. Differently, **1** was capable of penetrating deeply into the core of HeLa spheroids (up to 300 μm), as can be seen in **Figure 5B**. The internal structure of the spheroids was clearly illuminated. Moreover, **1** exhibited a stronger and clearer phosphorescence in the deeper sections of the spheroids under TP laser excitation compared with OP excitation, confirming the deeper tissue penetration and enhanced PDT efficiency of TP light compared with OP light.

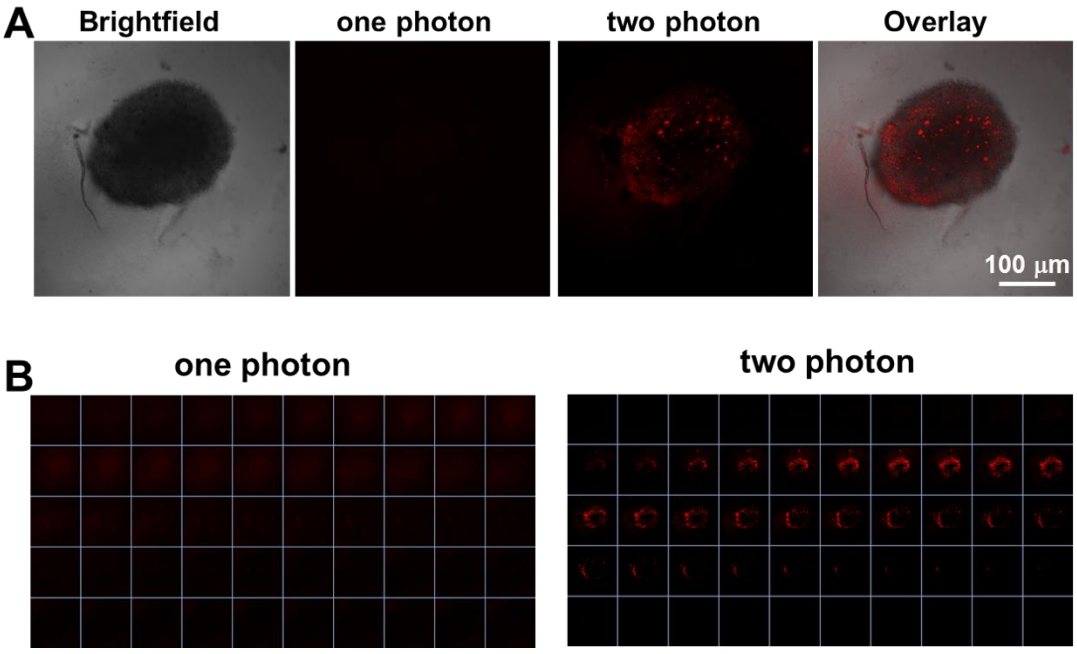

Figure 6. (A) 1P and 2P images of **2** (50 μM) after incubation with HeLa spheroids for 12 h. (B) Z-stack images of the same HeLa spheroids captured every 5 μm along the Z-axis. Excitation wavelengths:

10.1002/chem.201701392

800 nm (**1** and **2**), Emission filter: 600 ± 20 nm (for **1** and **2**).

Finally, we also investigated the cellular localization of Ru(II) complexes in HeLa cell monolayers after light treatment. The cellular localization of **1** changed after light irradiation, with the compound accumulating in the nucleus (**Figure 7B**). Similar re-localization results had been reported for other Ru(II) PSs.[10g, 39] Such an observation could be explained by the generation of singlet oxygen upon light irradiation, that damages the nuclear membrane and hence enables the penetration of **1** into the nucleus. On the contrary, **2** was still found to localise in the cell membranes after light irradiation (**Figure 7D**).

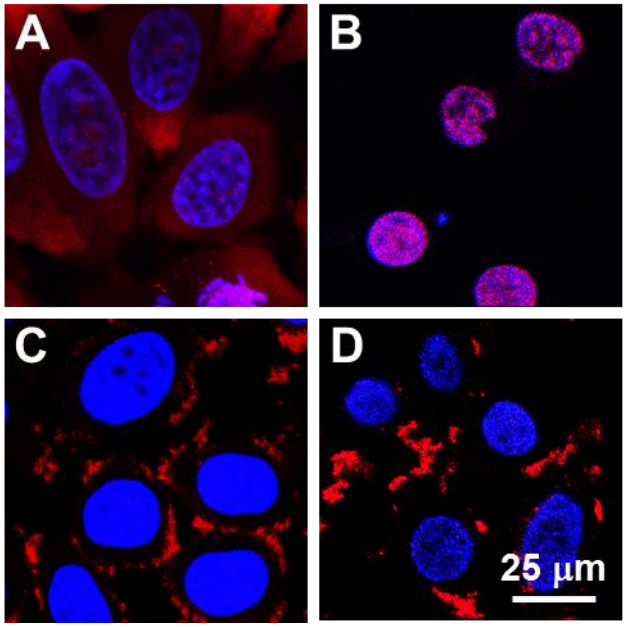

Figure 7. Confocal microscopy images showing the cellular localization of **1** (50 µM, 4 h) without light irradiation (A) and after irradiation (B). Confocal microscopy images showing the cellular localization of **2** (50 µM, 4 h) without light irradiation (C) and after irradiation (D). Excitation wavelengths: 458 nm (**1** and **2**), and 405 nm (Hoechst 33342). Emission filter: 600 ± 20 nm (for **1** and **2**), 460 ± 20 nm (for Hoechst 33342).

Conclusions

In this paper, we investigated the properties of two Ru(II) complexes in regard to their potential as photosensitizers for one- and two-photon PDT. The correlation between cellular localization and PDT efficiency was investigated. Although the structures of **1** and **2** are quite similar, significant differences in their biological properties were found. The unveiled cell-membrane affinity of **2** significantly reduced its dark toxicity compared to **1**, which was found to spread throughout cytoplasm and nucleus by microscopy imaging. The dark toxicity of **1** may thus arise from its ability to reach the nucleus, where it may interact with the DNA, as shown for other nucleus targeting Ru(II) complexes exhibiting strong anticancer activity.[19a] In the case of **2**, due to its poor cellular uptake ability, it was only detected at the cell membrane, where it may induce membrane damage on cancer cell monolayers upon photoactivation. In the case of the cancer cell spheroids, **2** only reached the outer shell of MCTSs, and irradiation did not result in oxidative damage to cells inside the spheroids. The cellular uptake ability of **1** was better than **2** even though **1** was less lipophilic than **2**. **1** could penetrate into HeLa MCTSs, similarly to the lysosome targeting Ru(II) polypyridyl complexes reported by our group before.[10] In this previous report, we showed that the investigated Ru(II) polypyridyl complexes can induce lysosome damage and re-localize towards the nucleus upon light irradiation. Similarly, we also observed accumulation of **1** in the nucleus after light irradiation, illustrating that severe oxidative damage occurred within the treated and irradiated cancer cells. Taken together, this study illustrates that small changes of the functional groups in polypyridyl Ru(II) complexes have a significant influence on their cellular localization as well as anticancer activity. This study

also confirms that MCTSs are a more ideal cancer cell model than cancer cell monolayer to mimic cellular uptake and tissue penetration on solid tumour.

Experimental Section

Instrumentations and Methods, ^{1}H and *^{13}C NMR spectra* were recorded in deuterated solvents on Bruker AV2-401, AV2-400, AV-500 and AV-501 at room temperature. The chemical shifts, δ, are reported in ppm (parts per million). The signals from the residual protons of deuterated solvent have been used as an internal reference.[40] The abbreviations for the peak multiplicities are as follows: s (singlet), d (doublet), dd (doublet of doublets), t (triplet), q (quartet), m (multiplet), and br (broad). Thin layer chromatography (TLC) was performed using silica gel 60 F-254 (Merck) plates with detection of spots being achieved by exposure to UV light. Column chromatography was performed using Silica gel 60 (0.040-0.063 mm mesh, Merck). Eluent mixtures are expressed as volume to volume (v/v) ratios. *ESI mass spectrometry* was performed using a Bruker Esquire 6000 spectrometer. In the assignment of the mass spectra, the most intense peak is listed. *Elemental microanalyses* were performed on a LecoCHNS-932 elemental analyser.

*Synthesis of 1,2-Dimethoxy-4,5-diaminobenzene (**1b**).* A solution of 1,2,-dimethoxy-4,5-dinitrobenzene (0.30 g, 1.33 mmol) in MeOH (100 mL) was reduced by hydrogenation using 5 bar of H_2, 20 mmol % of Pd/C (32 mg, 0.30 mmol) and a few drops of acetic acid. After 3 h, the catalyst was filtered off and the filtrated was concentrated *in vacuo*. The

crude product was purified by redissolving the residue in CH_2Cl_2 (50 mL) and extracted with 1M HCl solution (100 mL). The two phases were separated and the aqueous pink layer was adjusted to pH≈14 with solid NaOH pellets, which resulted in a colour change from pink to green. The aqueous layer was then extracted with CH_2Cl_2 (3 × 100 mL). The combined organic layers were dried over $MgSO_4$, filtered and evaporated to obtain 1,2-dimethoxy-4,5-diaminobenzene (**1b**) as a greenish oil, which was directly used without further purification for the next reaction step. Yield 91% (0.20 g, 1.21 mmol). The spectroscopic data match those previously reported by L. Perrin *et al*.[41]

*7,8-Dimethoxydipyrido[3,2-a:2`,3`-c]phenazine (dppz-7,8-(OMe)$_2$) (**1c**).* This ligand was synthesized by Schiff base condensation using an adapted procedure described by Aguirre *et al*.[42] A mixture of 1,2-dimethoxy-4,5-diaminobenzene (0.10 g, 0.59 mmol) and 1,10-phenantroline (0.08 g, 0.40 mmol) was refluxed in EtOH (30 mL) for approximately 4 h. The reaction was allowed to reach room temperature. The solvent was evaporated to leave only a few millilitres of EtOH and the residue was kept in the freezer until a brownish precipitate was formed. The solids were filtered off and washed with cold EtOH and then Et_2O to obtain 7,8–dimethoxydipyrido[3,2-a:2`,3`-c]phenzine (**1c**). Yield: 73% (0.15 g, 0.43 mmol). The spectroscopic data match those reported previously by Aguirre *et al*. [42]

*Synthesis of [Ru(phen)$_2$(dppz-7,8-(OMe)$_2$)][(PF$_6$)$_2$] (**1**).* [Ru(phen)$_2$Cl$_2$]·2H$_2$O (0.10 g, 0.18 mmol) and 7,8–dimethoxydipyrido-[3,2-a:2`,3`-c]phenazine (dppz-7,8-(OMe)$_2$ (**1c**), 0.075 g, 0.219 mmol) was refluxed under N_2 in a thoroughly deareated EtOH:H_2O (1:1, 30

mL) solution overnight. The solvent was evaporated *in vacuo*. The solid was redissolved in H_2O (5 mL) and NH_4PF_6 was added to precipitate the crude complex as a PF_6 salt. The crude product was further purified by silica column chromatography with CH_3CN/aq. KNO_3 0.4 M (10:1) as the eluent. The fractions containing the product were combined and the eluent was evaporated *in vacuo*. The reddish/orange residue was redissolved in CH_3CN (10 mL) to dissolve the product, while the white, insoluble solid (excess of KNO_3) was removed by filtration. The solvent was removed *in vacuo*, the solid redissolved in H_2O (15 mL) and addition of NH_4PF_6 allowed the precipitation of the product as a PF_6 salt. The precipitate was further washed with H_2O (3 × 30 mL) and freeze-dried to obtain $[Ru(phen)_2(dppz\text{-}7,8\text{-}(OMe)_2)][(PF_6)_2]$ (**1**) as a reddish powder. Yield: 60% (0.088 g, 0.110 mmol). ^{1}H NMR (400 MHz, CD_3CN): δ/ppm = 9.57-9.55 (m, 2H), 8.63-8.60 (m, 4H), 8.27 (s, 4H), 8.21-8.19 (m, 2H), 8.08-8.03 (m, 4H), 7.76-7.73 (m, 2H), 7.68-7.62 (m, 6H), 4.09 (s, 6H). ^{13}C NMR (125 MHz, CD_3CN): δ/ppm = 156.9, 154.5, 154.2, 154.0, 150.9, 149.0, 148.9, 142.4, 138.6, 138.0, 137.9, 134.0, 132.1, 132.1, 131.9, 129.2, 129.1, 127.9, 127.0, 126.9, 107.1, 57.5. ESI-MS: *m/z* (%) = 402.0 ($[M\text{-}2PF_6]^{2+}$, 100). Elemental Analysis: calcd. for $C_{44}H_{30}F_{12}N_8O_2P_2Ru(H_2O)_{2.5}$: C, 46.41; H, 3.10; N, 9.84. Found: C, 46.11; H, 2.88; N, 9.72.

*Synthesis of $[Ru(phen)_2(dppz\text{-}7,8\text{-}(OH)_2)][(PF_6)_2]$ (**2**).* This complex was synthesized by an adapted synthetic procedure described by Perrin *et al*.[41] A solution of $[Ru(phen)_2(dppz\text{-}7,8\text{-}(OH)_2)][(PF_6)_2]$ (**2,** 0.05 g, 0.046 mmol) in glacial acetic acid (3 mL) was stirred at 30 °C for 30 min. An aqueous solution of 48% HBr (9 mL) was slowly added and the

reaction mixture was heated to reflux overnight. The next morning, an additional 48% HBr solution (4.5 mL) was added and the reaction was kept at reflux for a further 12 h. The reaction was allowed to cool to room temperature. The crude reaction was filtered through a cotton plug and the solvent was reduced *in vacuo*. The residue was redissolved in CH_3CN (30 mL) and filtered again. The CH_3CN-solution containing the product was evaporated to dryness. The solid was redissolved in H_2O (15 mL) and 10 mL saturated NH_4PF_6 solution was added to precipitate the product as a PF_6 salt. The precipitate was further washed with H_2O (3 × 30 mL) and freeze-dried to obtain $[Ru(phen)_2(dppz\text{-}7,8\text{-}(OH)_2)][(PF_6)_2]$ (**2**) as a brownish solid. Yield: 33% (0.016 g, 0.015 mmol). ^{1}H NMR (400 MHz, CD_3CN): δ/ppm = 9.63-9.61 (m, 2H), 8.62-8.59 (m, 4H), 8.26 (s, 4H), 8.19-8.18 (m, 2H), 8.05-8.01 (m, 4H), 7.82 (s, 2H), 7.74-7.71 (m, 2H), 7.67-7.61 (m, 4H). ^{13}C NMR (125 MHz, CD_3CN): δ/ppm = 154.3, 154.2, 154.0, 153.7, 150.9, 149.0, 148.9, 142.2, 138.4, 137.9, 137.9, 134.0, 132.1, 132.1, 132.0, 129.1, 127.9, 127.0, 126.9, 110.0. ESI-MS: *m/z* (%) = 388.0 ($[M\text{-}2PF_6]^{2+}$, 100). Elemental Analysis: calcd. for $C_{42}H_{26}F_{12}N_8O_2P_2Ru(H_2O)_{2.5}$: C, 45.42; H, 2.81; N, 10.09. Found: C, 45.33; H, 3.16; N, 10.27.

X-ray crystallography. Single-crystal X-ray diffraction data were collected at low temperature (153(1) K for **1** and 183(1) K for **1c**) on a *SuperNova Atlas* area-detector diffractometer from *Rigaku Oxford Diffraction*[43] (formerly Agilent Technologies) using a single wavelength Enhance X-ray source with Cu K_α radiation (λ = 1.54184 Å) from a micro-focus X-ray source and an Oxford Instruments Cryojet XL cooler. The selected suitable single crystals were mounted using polybutene oil on a flexible loop fixed on a

goniometer head and immediately transferred to the diffractometer. Pre-experiment, data collection, data reduction and analytical absorption correction[44] were performed with the program suite *CrysAlis*^{Pro}.[1] The crystal structure of **1** was solved with *SHELXS97*[45] and refined with *SHELXL97*[3] using the *WinGX* program system[46] while the crystal structure of **1c** was solved with *SHELXT*[47] and refined with *SHELXL2014*[48] using the *Olex2* crystallographic software.[49] The *SQUEEZE*[50] method included in *PLATON*[51] was used to calculate the disordered solvent contribution to the calculated structure factors and to determine the number of isolated water molecules in the solvent-accessible regions. For more details about the data collection and refinements parameters, see Tables S1 and the CIF files (CCDC-1502934 (for **1**) and CCDC-1502935 (for **1c**) contain the supplementary crystallographic data for this paper. These data can be obtained free of charge from The Cambridge Crystallographic Data Centre via www.ccdc.cam.ac.uk/data_request/cif). Crystal data for **1.(ClO$_4$)$_2$.(H$_2$O)$_{32}$** (M = 1579.24 g/mol): tetragonal, space group $I4_1/a$ (no. 88), a = 30.4431(7) Å, c = 31.0134(9) Å, V = 28742.7(13) Å^3, Z = 16, T = 153(1) K, μ(CuKα) = 3.348 mm^{-1}, *Dcalc* = 1.460 g/cm^3, 39218 reflections measured ($4.1 \leq 2\Theta \leq 133.2$), 12614 unique ($R_{int}$ = 0.1204, R_{sigma} = 0.0816) which were used in all calculations. The final R_1 was 0.0975 (>2sigma(I)) and wR_2 was 0.2979 (all data). Crystal data for **1c.(CHCl$_3$)** (M = 461.72 g/mol): orthorhombic, space group $Pca2_1$ (no. 29), a = 18.5556(5) Å, b = 15.5691(5) Å, c = 7.06046(15) Å, V = 2039.73(10) Å^3, Z = 4, T = 183(1) K, μ(CuKα) = 4.298 mm^{-1}, *Dcalc* = 1.504 g/cm^3, 8546 reflections measured ($5.7 \leq 2\Theta \leq 136.3$), 2762 unique ($R_{int}$ = 0.0183, R_{sigma} = 0.0184) which were used in all calculations. The final R_1 was 0.0433 ($I > 2\sigma(I)$) and wR_2 was 0.1169 (all data).

10.1002/chem.201701392

Photophysical property measurements. UV/Vis absorption spectra and extinction coefficients were obtained on a Varian Cary 50 Scan UV/vis spectrophotometer using standard quartz cells with 1 cm path length. Emission spectra were recorded on an Edinburgh Instrument FLSP920 spectrometer equipped with a 450 W Xenon lamp, double monochromators for the excitation and emission pathways, and a red-sensitive photomultiplier (PMT-R928) as detector. The emission spectra were fully corrected by using the standard corrections supplied by the manufacturer for the spectral power of the excitation source and the sensitivity of the detector. The quantum yields were measured by use of an integrating sphere with an Edinburgh Instrument FLSP920 spectrometer. The absorbance of the samples was kept below 0.1 to avoid inner filter effects, except for the concentration-dependent measurements, and all measurements were carried out at 293 K. The luminescence lifetimes were measured by using a μF900 pulsed 60W xenon microsecond flash lamp with a repetition rate of 100 Hz and a multichannel scaling module. The emission was collected at right angles to the excitation source with the emission wavelength selected by using a double grated monochromator and detected by a R928-P PMT. The instrument response function (IRF) was measured by using the blank solvent as scattering sample and setting the monochromator at the emission wavelength of the excitation beam. The resulting intensity decay is a convolution of the luminescence decay with the IRF and iterative convolution of the IRF with a decay function and non-linear least-squares analysis was used to analyze the convoluted data

Singlet oxygen quantum yield measurement.[7c] An air-saturated acetonitrile solution, containing the complex (OD=0.1 at irradiation wavelength), p-nitrosodimethyl aniline (RNO, 24 μM), imidazole (12 mM) or an air-saturated PBS buffer solution, containing the complex (OD = 0.1 at irradiation wavelength), RNO (20 μM), histidine (10 mM) were irradiated in a luminescence quartz cuvette at 420 nm in a RPR100 Rayonet chamber reactor (Southern New England Ultraviolet Company) complete with six lamps, at different time intervals. The absorbance of the solution was then evaluated. Plots of variations in absorbance at 440 nm in PBS or at 420 nm in acetonitrile (A_0–A, where A_0 is the absorbance before irradiation) versus the irradiation times for each sample were prepared and the slope of the linear regression was calculated (S_{sample}). As a reference compound, phenalenone (Φ_{ref} ($^1O_2$) = 95 %) was used in both methods, to obtain S_{ref} Equation (1) was applied to calculate the singlet oxygen quantum yields (Φ_{sample}) for every sample:

$$\Phi_{sample} = \Phi_{ref} * S_{sample}/S_{ref} * I_{ref} / I_{sample} \quad (1)$$

$$I = I_0 * (1 - 10^{-A_\lambda}) \quad (2)$$

I (absorbance correction factor) was obtained with Equation (2), where I_0 is the light intensity of the irradiation source in the irradiation interval and A_λ is the absorbance of the sample at wavelength λ.

Determination of two-photon absorption cross sections. The two-photon absorption spectra of the probes were determined over a broad spectral region by the typical two-photon induced luminescence (TPL) method relative to Rhodamine B in methanol as the standard. The two-photon luminescence data were acquired using an Opolette™ 355II

(pulse width ≤ 100 fs, 80 MHz repetition rate, tuning range 720-850 nm, Spectra Physics Inc., USA). Two-photon luminescence measurements were performed in fluorometric quartz cuvettes. The experimental luminescence excitation and detection conditions were conducted with negligible reabsorption processes, which can affect TPA measurements. The quadratic dependence of two-photon induced luminescence intensity on the excitation power was verified at an excitation wavelength of 800 nm. The two-photon absorption cross section of the probes was calculated at each wavelength according to equation (1).[52]

$$\delta_2 = \delta_1 \frac{\phi_1 C_1 I_2 n_2}{\phi_2 C_2 I_1 n_1} \quad (3)$$

where I is the integrated luminescence intensity, C is the concentration, n is the refractive index, and Φ is the quantum yield. Subscript '1' stands for reference samples, and '2' stands for samples.

Log P Measurements. Log P is the partition coefficient between octanol and water determined by the flask-shaking method.[23a] An aliquot of a stock solution of **1** and **2** in H_2O was added to an equal volume of octanol (saturated with 0.9% NaCl w/v) respectively. The mixture was shaken overnight at 60 rpm at 298 K to allow partitioning. After the sample was centrifuged at 3000 rpm for 10 min, the aqueous layer was carefully separated from the octanol layer for ruthenium analysis. The Ru concentration in the aqueous phase was determined by UV-vis spectra and used to calculate the $[Ru]_o/[Ru]_w$ ratio.

Cell Lines and Cell Culture. Cervical cancer HeLa cells were maintained in DMEM (Gibco) with fetal calf serum (FCS, 5 %; Gibco), penicillin (100 U mL^{-1}), streptomycin

(100 mg mL^{-1}) in a humidified atmosphere at 37 °C and 5 % CO_2. Normal lung fibroblast (MRC-5) cells were cultured in F-10 medium (Gibco) supplemented with FCS (10 %; Gibco), penicillin (100 U mL^{-1}), streptomycin (100 mg mL^{-1}) in a humidified atmosphere at 37 °C and 5 % CO_2

Dark- and photo-toxicity on cell monolayer.[23a] A fluorometric cell viability assay using resazurin (Promocell GmbH) was used to compare the cytotoxicity of the ruthenium complexes in the dark and upon UV irradiation. HeLa cells were plated in triplicates in 96-well plates at a density of 4000 cells per well in 100 μL, 24 h prior to treatment. MRC-5 cells were plated in triplicates in 96-well plates at a density of 7500 cells per well in 100 μL, 24 h prior to treatment. For dark treatment, the cells were exposed to increasing concentration of the compounds for 4 h. This was followed by 44 h incubation in the dark. For phototoxicity study, cells were treated for 4 h with increasing concentrations of the compounds in the dark. After that, the medium was removed and replaced by fresh culture medium prior to 20 min irradiation at 420 nm (20 min, 9.27 J cm^{-2}) in a RPR200 Rayonet chamber reactor (Southern New England Ultraviolet Company). After 44 h in the incubator, the medium was replaced by 100 μL complete medium containing resazurin (final concentration 0.2 mg mL^{-1}). After 4 h incubation at 37 °C, fluorescence intensity of the highly red fluorescent resorufin product was quantified at 590 nm emission with 540 nm excitation wavelength in a SpectraMax M5 microplate reader. Light doses were evaluated with a Gigahertz Optic X1-1 optometer.

Generation and analysis of 3D HeLa MCTSs. MCTSs were cultured using the liquid overlay method.[53] HeLa cells in the exponential growth phase were dissociated by a trypsin/EDTA solution to gain single-cell suspensions. A number of 2500 diluted HeLa cells were transferred to 1.5% agarose-coated transparent 96-well plates with 200 μL of Dulbecco's modified Eagle medium (DMEM) containing 10% serum. The single cells would generate MCTSs approximately 400 μm in diameter at day 4 with 5% CO_2 in air at 37 °C.

Photo-cytotoxicity test on 3D MCTSs.[10g] For MCTSs, HeLa MCTSs of diameters around 400 μm were treated by carefully replacing 50% of the medium with drug supplemented standard medium (**1**, **2**, 5-ALA and cisplatin) using an eight-channel pipet. In parallel, for the untreated reference MCTS, 50% of medium of the solvent-containing or solvent-free medium were replaced. Four MCTS were treated per condition and drug concentration, and the DMSO volume was less than 0.5% (v/v). After incubation in the dark for 24 h, MCTSs were exposured to irradiation. For OP-PDT (450 nm, 10.0 $J{\cdot}cm^{-2}$) HeLa MCTSs were irradiated by a Zolix MLED4 surface LED light source (10 mW cm^{-2}) for 1000 s. For TP-PDT (800 nm, 9.90 $J{\cdot}cm^{-2}$), HeLa MCTSs was irradiated by a 800 nm two photon laser source equipped in LSM 710 Carl Zeiss laser scanning confocal microscope (30 mW cm^{-2}) for 330 s. treatments were conducted in this experiment. The MCTSs were then allowed to incubate for another 48 h. The cytotoxicity of ruthenium complexes toward MCTSs was measured by ATP concentration with CellTiter-Glo® 3D Cell Viability kit (Promega, USA). After 60 min of incubation, MCTSs were carefully

transferred into black-sided, flat-bottomed 96-well plates (Corning) and pipet-mixed for luminescence measurement on infinite M200 PRO equipment (TECAN).

ICP-MS Assay.[23a] ICP-MS measurements were performed on an Agilent QQQ 8800 Triple quad ICP-MS spectrometer (Agilent Technologies) with a ASX200 autosampler (Agilent Technologies), equipped with standard nickel cones and a "micro-mist" quartz nebulizer fed with 0.3 ml/min analytic flow (as a 2% HNO_3 aqueous solution). Ruthenium was measured against a Ru single element standard (Merck 170347) and verified by a control (Agilent5188-6524 PA Tuning 2). Ruthenium content of the samples was determined by means of a 8-step serial dilution in the range between 0 and 200 ppb in Ru (R>1.00) with a background equivalent concentration of BEC: 14.4 ppt and a detection limit of DL: 5.4 ppt. The isotope Ru^{99} (12.76% abundance) ^{101}Ru (17.06% abundance) was evaluated in "no-gas" mode and He-gas mode. Spiking the samples with 1% methanol (to account for eventual carbon content from the biological samples) resulted in equivalent values within error ranges. A solution of Indium (500 ppb) and Tungsten (500 ppb) was used as internal standard. The results are expressed as ppb Ru / sample. Data were reported as the means standard deviation (n = 3).

Cell imaging. Cellular localization of the luminescent ruthenium complexes was assessed by fluorescence microscopy. For cell monolayer imaging, HeLa cells were grown on 35 mm glass bottom dishes (Greiner) in 3 mL complete DMEM cell culture medium at a density of 1×10^5 cells per mL 24 h prior to drug treatment. For dark treatment, the cells

were incubated with **1** or **2** for 4 h at a concentration of 50 μM. For spheroids imaging, HeLa MCTSs were firstly incubated with **1** or **2** for 12 h at a concentration of 50 μM. The cells were then imaged by a CLSM microscope (LSM 710, Carl Zeiss, Göttingen, Germany). The one- and two-photon excitation wavelengths were 458 nm and 800 nm, respectively; emission filter: 600 ± 20 nm.

Cellular localization. Cellular localization of the luminescent ruthenium complexes was assessed by fluorescence microscopy. HeLa cells were grown on 35 mm glass bottom dishes (Greiner) in 3 mL DMEM cell culture complete medium at a density of 1×10^5 cells per mL 24 h prior to drug treatment. The cells were incubated with **1** or **2** for 4 h at a concentration of 50 μM. Cells were then co-incubated about half an hour with mitochondrial dye mitotracker green (MTG) and nucleus dye Hoechst 33342 (for **1**) or green cell membrane dye Dio and nucleus dye Hoechst 33342 (for **2**) respectively according to manufacturer's instructions (Molecular Probes™, Life technology). The cells were then washed with 1× PBS 3 times prior to imaging by a CLSM microscope (LSM 710, Carl Zeiss, Göttingen, Germany). Excitation wavelengths: 458 nm (**1** and **2**,), 488 nm (Dio), 488 nm (MTG green) and 405 nm (Hoechst 33342). Emission filter: 600 ± 20 nm (for **1** and **2**), 520 ± 20 nm (for MTG), 500 ± 20 nm (Dio) and 460 ± 20 nm (for Hoechst 33342).

Cellular localization after PDT. For cellular localization after PDT treatment, the cells were incubated with **1** or **2** for 4 h at a concentration of 50 μM and then replaced with fresh

medium 10 min before irradiation (420 nm, 20 min, 9.27 J cm^{-2}). After light treatment, cells were left in the dark for 1 h recovery and then stained with Hoechst 33342 (1 μg/mL) for 30 min. Cells were then washed with PBS prior to imaging by a CLSM Leica SP5 Mid UV-VIS Leica microscope. The excitation wavelengths for **1** and **2** were 458 nm while the excitation wavelength of Hoechst 33342 is 405 nm. Emission filter: 600 ± 20 nm (for **1** and **2**), 460 ± 20 nm (for Hoechst 33342).

Human plasma stability.[8a, 54] A recently described procedure by Gasser and co-workers was adapted to perform the stability experiment of complex **1** and **2**. Diazepam was obtained from Sigma-Aldrich and used as the internal standard. The human plasma was provided by the Blutspendezentrum Zürich, Switzerland. For each experiment, fresh stock solutions of **1** (1.6 mM), **2** (5.0 mM) and diazepam (800 μM) were prepared in DMSO and kept protected from light.

To 975 μL of plasma, 12.5 μL of the respective solution containing the compound to be studied (**1** (1.6 mM) or **2** (5.0 mM)) and 12.5 μL diazepam solution were added to a total volume of 1000 μL. The resulting aqueous solutions were incubated for 0 h, 24 h and 48 h at 37 °C with continuous and gentle shaking (ca. 700 rpm) while protected from light. Afterwards, the plasma solution was quenched with 4 mL CH_2Cl_2 and the mixture was shaken for 5 min at room temperature followed by centrifugation at 3000 U/min for 10 min. The organic layer was separated from the aqueous layer and dried by a gentle stream of nitrogen. The obtained residue was redissolved in 80 μL of a 8/5 (v/v) CH_3CN/H_2O mixture containing 0.02% TFA and 0.05% HCOOH. 5 μL of the solution was injected into the

UPLC (Acquity Ultra Performance LC, Waters) that was connected to a mass spectrometer (Bruker Esquire 6000) operated in ESI mode. An Acquity UPLC BEH C18 (2.1 × 50 mm) was used as a reverse phase column and was used with a flow rate of 0.6 mL min^{-1}. The UV absorption was measured at 375 nm. The runs were performed with a linear gradient of A (acetonitrile (Sigma-Aldrich HPLC grade) and B (distilled water containing 0.02% TFA and 0.05% HCOOC): t = 0 – 1 min, 1% A; t = 1.5 min, 2% A; t = 4 – 5 min, 100% A.

Supporting information

^{1}H and ^{13}C NMR spectra of **1** and **2**, ESI-MS spectra of **1** and **2**, crystal data for **1c** and **1**, ORTEP plot of **1c**, UV-Vis spectra of **1** and **2**, emission spectra of **1** and **2**, lifetime spectra of **1** and **2**, integrated emission intensity for **1** and **2**, UPLC traces of **1** and **2**.

Author information

Corresponding Authors:

* E-mail: ceschh@mail.sysu.edu.cn (H.C.)

* E-mail: gilles.gasser@chimie-paristech.fr (G.G.)

* Website: www.gassergroup.com (G.G.)

Conflict of interest

The authors declare no conflict of interest.

10.1002/chem.201701392

Acknowledgements

This work was financially supported by the Swiss National Science Foundation (Professorships No. PP00P2_133568 and PP00P2_157545 to G.G), the University of Zurich (G.G), the 973 program (No. 2015CB856301 to H. C.), the National Science Foundation of China (Nos. 21471164 and 21525105 to H. C.) and the China Scholarships Council (Grant No. 201506380026 to H. H.). This work has received support under the program «Investissements d'Avenir » launched by the French Government and implemented by the ANR with the reference ANR-10-IDEX-0001-02 PSL (G.G.). The authors thank the Center for Microscopy and Image Analysis of the University of Zurich for access to state-of-the-art equipment.

10.1002/chem.201701392

Table of Contents

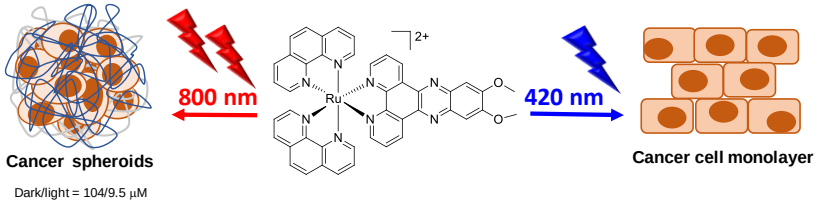

The Structure influences the Activity! Two Ru(II) polypyridyl complexes have been synthesized, characterized and investigated as photosensitizers (PSs) for photodynamic therapy (PDT) against cancer.

References

[1] D. E. J. G. J. Dolmans, D. Fukumura and R. K. Jain, *Nat. Rev. Cancer* **2003**, *3*, 380-387.

[2] B. W. Henderson and T. J. Dougherty, *Photochem. Photobiol.* **1992**, *55*, 145-157.

[3] A. P. Castano, T. N. Demidova and M. R. Hamblin, *Photodiagn. Photodyn. Ther.* **2004**, *1*, 279-293.

[4] A. Naik, R. Rubbiani, G. Gasser and B. Spingler, *Angew. Chem. Int. Ed.* **2014**, *126*, 7058-7061.

[5] B. Mao, Y. Ji, M. Fañanás-Mastral, G. Caroli, A. Meetsma and B. L. Feringa, *Angew. Chem. Int. Ed.* **2012**, *51*, 3168-3173.

[6] S. B. Brown, E. A. Brown and I. Walker, *Lancet Oncol.* **2004**, *5*, 497-508.

[7] a) L. K. McKenzie, I. V. Sazanovich, E. Baggaley, M. Bonneau, V. Guerchais, J. A. G. Williams, J. A. Weinstein and H. E. Bryant, *Chem. Eur. J.* **2016**, *23*, 234-238; b) T. Wang, N. Zabarska, Y. Wu, M. Lamla, S. Fischer, K. Monczak, D. Y. W. Ng, S. Rau and T. Weil, *Chem. Comm.* **2015**, *51*, 12552-12555; c) A. Leonidova, V. Pierroz, R. Rubbiani, J. Heier, S. Ferrari and G. Gasser, *Dalton Trans.* **2014**, *43*, 4287; d) A. Leonidova and G. Gasser, *ACS Chem. Biol.* **2014**, *9*, 2180-2193; e) S. Bonnet, *Comments Inorg. Chem* **2015**, *35*, 179-213; f) Y. Chen, R. Guan, C. Zhang, J. Huang, L. Ji and H. Chao, *Coord. Chem. Rev.* **2016**, *310*, 16-40; g) C. Mari, V. Pierroz, S. Ferrari and G. Gasser, *Chem. Sci.* **2015**, *6*, 2660-2686; h) C. Mari and G. Gasser, *CHIMIA* **2015**, *69*, 176-181; i) J. D. Knoll and C. Turro, *Coord. Chem. Rev.* **2015**, *282,Äì283*, 110-126.

[8] a) V. Pierroz, T. Joshi, A. Leonidova, C. Mari, J. Schur, I. Ott, L. Spiccia, S. Ferrari and G. Gasser, *J. Am. Chem. Soc.* **2012**, *134*, 20376-20387; b) V. Fernandez-Moreira, F. L. Thorp-Greenwood and M. P. Coogan, *Chem. Comm.* **2010**, *46*, 186-202; c) N. P. Cook, V. Torres, D. Jain and A. A. Marti, *J. Am. Chem. Soc.* **2011**, *133*, 11121-11123; d) M. R. Gill and J. A. Thomas, *Chem. Soc. Rev.* **2012**, *41*, 3179-3192.

[9] G. Shi, S. Monro, R. Hennigar, J. Colpitts, J. Fong, K. Kasimova, H. Yin, R. DeCoste, C. Spencer, L. Chamberlain, A. Mandel, L. Lilge and S. A. McFarland, *Coord. Chem. Rev.* **2015**, *282- 283*, 127-138.

[10] a) T. Joshi, V. Pierroz, C. Mari, L. Gemperle, S. Ferrari and G. Gasser, *Angew. Chem. Int. Ed.* **2014**, *53*, 2960-2963; b) H. Huang, P. Zhang, B. Yu, C. Jin, L. Ji and H. Chao, *Dalton Trans.* **2015**, *44*, 17335-17345; c) B. A. Albani, B. Pena, N. A. Leed, N. A. B. G. de Paula, C. Pavani, M. S. Baptista, K. R. Dunbar and C. Turro, *J. Am. Chem. Soc.* **2014**, *136*, 17095-17101; d) B. S. Howerton, D. K. Heidary and E. C. Glazer, *J. Am. Chem. Soc.* **2012**, *134*, 8324-8327; e) P. M. Keane, F. E. Poynton, J. P. Hall, I. V. Sazanovich, M. Towrie, T. Gunnlaugsson, S. J. Quinn, C. J. Cardin and J. M. Kelly, *Angew. Chem. Int. Ed.* **2015**, *54*, 8364-8368; f) V. H. S. van Rixel, B. Siewert, S. L. Hopkins, S. H. C. Askes, A. Busemann, M. A. Siegler and S. Bonnet, *Chem. Sci.* **2016**, *7*, 4922-4929; g) H. Huang, B. Yu, P. Zhang, J. Huang, Y. Chen, G. Gasser, L. Ji and H. Chao, *Angew. Chem. Int. Ed.* **2015**, *54*, 14049-14052.

[11] a) A. V. Kachynski, PlissA, A. N. Kuzmin, T. Y. Ohulchanskyy, A. Baev, J. Qu and P. N. Prasad, *Nat. Photon.* **2014**, *8*, 455-461; b) S. Chakrabortty, B. K. Agrawalla, A. Stumper, N. M. Vegi, S. Fischer, C. Reichardt, M. Kögler, B. Dietzek, M. Feuring-Buske, C. Buske, S. Rau and T. Weil, *J. Am. Chem. Soc.* **2017**, *139*, 2512-2519.

[12] J. D. Bhawalkar, N. D. Kumar, C. F. Zhao and P. N. Prasad, *J. Clin. Laser Med. Surg.* **1997**, *15*, 201-204.

[13] a) A. Karotki, M. Khurana, J. R. Lepock and B. C. Wilson, *Photochem. Photobiol.* **2006**, *82*, 443-452; b) M. Drobizhev, Y. Stepanenko, Y. Dzenis, A. Karotki, A. Rebane, P. N. Taylor and H. L. Anderson, *J. Am. Chem. Soc.* **2004**, *126*, 15352-15353; c) M. Drobizhev, Y. Stepanenko, A. Rebane, C. J. Wilson, T. E. O. Screen and H. L. Anderson, *J. Am. Chem. Soc.* **2006**, *128*, 12432-12433; d) M. Pawlicki, H. A.

Collins, R. G. Denning and H. L. Anderson, *Angew. Chem. Int. Ed.* **2009**, *48*, 3244-3266.
[14] a) S. C. Boca, M. Four, A. Bonne, B. van der Sanden, S. Astilean, P. L. Baldeck and G. Lemercier, *Chem. Comm.* **2009**, 4590-4592; b) F. N. Castellano, H. Malak, I. Gryczynski and J. R. Lakowicz, *Inorg. Chem.* **1997**, *36*, 5548-5551; c) J. Liu, Y. Chen, G. Li, P. Zhang, C. Jin, L. Zeng, L. Ji and H. Chao, *Biomaterials* **2015**, *56*, 140-153; d) C. Feuvrie, O. Maury, H. Le Bozec, I. Ledoux, J. P. Morrall, G. T. Dalton, M. Samoc and M. G. Humphrey, *J. Phys. Chem. A* **2007**, *111*, 8980-8985.
[15] a) C. Girardot, G. Lemercier, J. C. Mulatier, J. Chauvin, P. L. Baldeck and C. Andraud, *Dalton Trans.* **2007**, 3421-3426; b) N. Z. Knezevic, V. Stojanovic, A. Chaix, E. Bouffard, K. E. Cheikh, A. Morere, M. Maynadier, G. Lemercier, M. Garcia, M. Gary-Bobo, J.-O. Durand and F. Cunin, *J. Mat. Chem. B* **2016**, *4*, 1337-1342; c) C. Girardot, B. Cao, J.-C. Mulatier, P. L. Baldeck, J. Chauvin, D. Riehl, J. A. Delaire, C. Andraud and G. Lemercier, *ChemPhysChem* **2008**, *9*, 1531-1535; d) M. Four, D. Riehl, O. Mongin, M. Blanchard-Desce, L. M. Lawson-Daku, J. Moreau, J. Chauvin, J. A. Delaire and G. Lemercier, *ChemPhysChem* **2011**, *13*, 17304-17312; e) G. Bœuf, G. V. Roullin, J. Moreau, L. Van Gulick, N. Zambrano Pineda, C. Terryn, D. Ploton, M. C. Andry, F. Chuburu, S. Dukic, M. Molinari and G. Lemercier, *ChemPlusChem* **2014**, *79*, 171-180.
[16] L. H. Hurley, *Nat. Rev. Cancer* **2002**, *2*, 188-200.
[17] M. Eriksson, M. Leijon, C. Hiort, B. Norden and A. Graeslund, *J. Am. Chem. Soc.* **1992**, *114*, 4933-4934.
[18] A. E. Friedman, J. C. Chambron, J. P. Sauvage, N. J. Turro and J. K. Barton, *J. Am. Chem. Soc.* **1990**, *112*, 4960-4962.
[19] a) H. Huang, P. Zhang, B. Yu, Y. Chen, J. Wang, L. Ji and H. Chao, *J. Med. Chem* **2014**, *57*, 8971-8983; b) H. Huang, P. Zhang, H. Chen, L. Ji and H. Chao, *Chem. Eur. J.* **2015**, *21*, 715-725; c) C. Tan, S. Lai, S. Wu, S. Hu, L. Zhou, Y. Chen, M. Wang, Y. Zhu, W. Lian, W. Peng, L. Ji and A. Xu, *J. Med. Chem* **2010**, *53*, 7613-7624.
[20] U. Schatzschneider, J. Niesel, I. Ott, R. Gust, H. Alborzinia and S. Wölfl, *ChemMedChem* **2008**, *3*, 1104-1109.
[21] H. Yin, M. Stephenson, J. Gibson, E. Sampson, G. Shi, T. Sainuddin, S. Monro and S. A. McFarland, *Inorg. Chem.* **2014**, *53*, 4548-4559.
[22] I. Haq, P. Lincoln, D. Suh, B. Norden, B. Z. Chowdhry and J. B. Chaires, *J. Am. Chem. Soc.* **1995**, *117*, 4788-4796.
[23] a) C. Mari, V. Pierroz, R. Rubbiani, M. Patra, J. Hess, B. Spingler, L. Oehninger, J. Schur, I. Ott, L. Salassa, S. Ferrari and G. Gasser, *Chem. Eur. J.* **2014**, *20*, 14421-14436; b) T. Joshi and G. Gasser, *Synlett* **2015**, *26*, 275-284.
[24] J. V. Caspar and T. J. Meyer, *J. Am. Chem. Soc.* **1983**, *105*, 5583-5590.
[25] H. Ishida, S. Tobita, Y. Hasegawa, R. Katoh and K. Nozaki, *Coord. Chem. Rev.* **2010**, *254*, 2449-2458.
[26] E. J. C. Olson, D. Hu, A. H √ ∂rmann, A. M. Jonkman, M. R. Arkin, E. D. A. Stemp, J. K. Barton and P. F. Barbara, *J. Am. Chem. Soc.* **1997**, *119*, 11458-11467.
[27] A. Frei, R. Rubbiani, S. Tubafard, O. Blacque, P. Anstaett, A. Felgenträger, T. Maisch, L. Spiccia and G. Gasser, *J. Med. Chem* **2014**, *57*, 7280-7292.
[28] I. Kraljic and S. E. Mohsni, *Photochem. Photobiol.* **1978**, *28*, 577-581.
[29] R. Schmidt, C. Tanielian, R. Dunsbach and C. Wolff, *J. Photochem. Photobiol., A* **1994**, *79*, 11-17.
[30] C. A. Puckett and J. K. Barton, *J. Am. Chem. Soc.* **2006**, *129*, 46.
[31] a) M. H. Gold and M. P. Goldman, *Dermatologic Surgery* **2004**, *30*; b) J. C. Kennedy, S. L. Marcus

and R. H. Pottier, *J. Clin. Laser Med. Surg.* **1996**, *14*, 289-304.
[32] a) W. Stummer, S. Stocker, A. Novotny, A. Heimann, O. Sauer, O. Kempski, N. Plesnila, J. Wietzorrek and H. J. Reulen, *J. Photochem. Photobiol., B* **1998**, *45*, 160-169; b) J. Moan, G. Streckyte, S. Bagdonas, Ø. Bech and K. Berg, *Int. J. Cancer* **1997**, *70*, 90-97.
[33] H. Tseng, J. A. Gage, T. Shen, W. L. Haisler, S. K. Neeley, S. Shiao, J. Chen, P. K. Desai, A. Liao, C. Hebel, R. M. Raphael, J. L. Becker and G. R. Souza, *Sci. Rep.* **2015**, *5*, 13987.
[34] a) A. Abbott, *Nature* **2003**, *424*, 870-872; b) J. L. Horning, S. K. Sahoo, S. Vijayaraghavalu, S. Dimitrijevic, J. K. Vasir, T. K. Jain, A. K. Panda and V. Labhasetwar, *Mol. Pharm.* **2008**, *5*, 849-862; c) S. Ghosh, G. C. Spagnoli, I. Martin, S. Ploegert, P. Demougin, M. Heberer and A. Reschner, *J. Cell. Physiol.* **2005**, *204*, 522-531; d) P. C. De Witt Hamer, A. A. G. Van Tilborg, P. P. Eijk, P. Sminia, D. Troost, C. J. F. Van Noorden, B. Ylstra and S. Leenstra, *Oncogene* **2007**, *27*, 2091-2096; e) C. Fischbach, R. Chen, T. Matsumoto, T. Schmelzle, J. S. Brugge, P. J. Polverini and D. J. Mooney, *Nat. Methods* **2007**, *4*, 855-860.
[35] J. Friedrich, C. Seidel, R. Ebner and L. A. Kunz-Schughart, *Nat. Protoc.* **2009**, *4*, 309-324.
[36] C. A. Puckett, R. J. Ernst and J. K. Barton, *Dalton Trans.* **2010**, *39*, 1159-1170.
[37] F. R. Svensson, M. Matson, M. Li and P. Lincoln, *Biophys. Chem.* **2010**, *149*, 102-106.
[38] a) S. Imstepf, V. Pierroz, R. Rubbiani, M. Felber, T. Fox, G. Gasser and R. Alberto, *Angew. Chem. Int. Ed.* **2016**, *55*, 2792-2795; b) G. Gasser, S. Neumann, I. Ott, M. Seitz, R. Heumann and N. Metzler-Nolte, *Eur. J. Inorg. Chem.* **2011**, *2011*, 5471-5478; c) S. Imstepf, V. Pierroz, P. Raposinho, M. Bauwens, M. Felber, T. Fox, A. B. Shapiro, R. Freudenberg, C. l. Fernandes, S. Gama, G. Gasser, F. Motthagy, I. R. Santos and R. Alberto, *Bioconjugate Chem.* **2015**, *26*, 2397-2407.
[39] J. X. Zhang, J. W. Zhou, C. F. Chan, T. C. K. Lau, D. W. J. Kwong, H. L. Tam, N. K. Mak, K. L. Wong and W. K. Wong, *Bioconjugate Chem.* **2012**, *23*, 1623.
[40] H. E. Gottlieb, V. Kotlyar and A. Nudelman, *J. Org. Chem.* **1997**, *62*, 7512-7515.
[41] L. Perrin and P. Hudhomme, *Eur. J. Org. Chem.* **2011**, *2011*, 5427-5440.
[42] J. D. Aguirre, H. T. Chifotides, A. M. Angeles-Boza, A. Chouai, C. Turro and K. R. Dunbar, *Inorg. Chem.* **2009**, *48*, 4435-4444.
[43] Y. Rigaku Oxford Diffraction, Oxfordshire, England, **2015**.
[44] R. C. Clark and J. S. Reid, *Acta Crystallogr., Sect. A* **1995**, *51*, 887-897.
[45] G. Sheldrick, *Acta Cryst.* **2008**, *64*, 112-122.
[46] L. Farrugia, *J. Appl. Cryst.* **2012**, *45*, 849-854.
[47] G. Sheldrick, *Acta Cryst.* **2015**, *A71*, 3-8.
[48] G. M. Sheldrick, *Acta Cryst.* **2015**, *C71*, 3-8.
[49] O. V. Dolomanov, L. J. Bourhis, R. J. Gildea, J. A. K. Howard and H. Puschmann, *J. Appl. Cryst.* **2009**, *42*, 339-341.
[50] A. Spek, *Acta Cryst.* **2015**, *C71*, 9-18.
[51] A. Spek, *Acta Cryst.* **2009**, *D65*, 148-155.
[52] C. Xu and W. W. Webb, *J. Opt. Soc. Am. B* **1996**, *13*, 481-491.
[53] H. Huang, P. Zhang, Y. Chen, L. Ji and H. Chao, *Dalton Trans.* **2015**, *44*, 15602-15610.
[54] M. Patra, K. Ingram, V. Pierroz, S. Ferrari, B. Spingler, R. B. Gasser, J. Keiser and G. Gasser, *Chem. Eur. J.* **2013**, *19*, 2232-2235.